IIETA International Information and Engineering Technology Association
Advancing the World of Information and Engineering

Mathematical Modelling of Engineering Problems
Vol. 13, No. 1, January, 2026, pp. 78-86
Journal homepage: http://iieta.org/journals/mmep

Human Detection and Tracking in Frequency Modulated Continuous Wave Radar Point Clouds Using Adaptive Density-Based Spatial Clustering of Applications with Noise

Fadhil Muhammad[1], Istiqomah[1,2*], Fiky Y. Suratman[1,2]

[1] School of Electrical Engineering, Telkom University, Bandung 40257, Indonesia
[2] Center of Excellence Intelligent Sensing–IoT, Telkom University, Bandung 40257, Indonesia

Corresponding Author Email: Istiqomah@telkomuniversity.ac.id

https://doi.org/10.18280/mmep.130108

Received: 9 October 2025
Revised: 27 November 2025
Accepted: 5 December 2025
Available online: 28 February 2026

Keywords:
Frequency Modulated Continuous Wave radar, human tracking, surveillance system, Density-Based Spatial Clustering of Applications with Noise, extended Kalman filter, point cloud, real-time

ABSTRACT

Frequency Modulated Continuous Wave (FMCW) radar offers strong potential for outdoor human tracking. However, its performance is affected by range-dependent variations in point cloud density and instability in position estimates, particularly at longer distances. Previous studies commonly employed Density-Based Spatial Clustering of Applications with Noise (DBSCAN) with fixed parameters, which resulted in reduced clustering accuracy under such conditions. To address this limitation, this study proposes a human tracking system based on the IWR6843ISK radar that integrates an adaptive DBSCAN scheme with a Kalman filter. The adaptive method divides the measurement space into distance zones and assigns DBSCAN parameters according to the density characteristics of each zone. Experimental results show that the proposed approach maintains cluster consistency at medium ranges. The Cluster Count Accuracy remains above 80% before degrading at farther distances due to lower Signal-to-Noise Ratio and point loss. The Kalman filter further stabilizes centroid trajectories by smoothing frame-to-frame variations and producing more coherent position estimates. Overall, the combination of adaptive DBSCAN and the Kalman filter enables reliable real-time human tracking within the radar's effective operating range. The proposed approach provides an efficient and practical solution for radar-based surveillance in outdoor environments.

1. INTRODUCTION

Surveillance systems play a vital role in various applications, particularly for human tracking in outdoor public environments. One important function is crowd management, which involves real-time monitoring and analysis of people's movements to ensure public safety and security [1]. Among the sensing technologies used for surveillance, Frequency Modulated Continuous Wave (FMCW) radar has emerged as a promising solution due to its ability to detect, track, and identify objects with high precision through electromagnetic wave reflections [2, 3]. FMCW radar offers key advantages, including reliable operation under diverse environmental conditions and accurate estimation of target position, velocity, and movement direction. These capabilities make it an ideal choice for modern surveillance systems that require both robustness and adaptability [4, 5].

Despite these advantages, deploying FMCW radar for human tracking in real-world environments presents several technical challenges. One major issue is the occurrence of ghost targets, false detections caused by multipath reflections, which can lead to inaccurate tracking [2]. Moreover, target tracking is often disrupted by occlusion and measurement noise, reducing both the accuracy and reliability of the system [6]. These challenges highlight the need for advanced processing techniques capable of distinguishing true targets from environmental clutter while maintaining consistent tracking performance in real-time [7].

Recent studies have explored various approaches to improve human tracking with mmWave FMCW radar. Techniques such as density-based clustering, ghost target mitigation, and multi-target tracking have been applied to radar point cloud data, yielding promising results in controlled or semi-structured environments [6, 8, 9]. While these methods demonstrate the capability of radar-based systems to track multiple individuals with reasonable accuracy, their performance often degrades in unstructured outdoor scenarios. This gap underscores the need for a tracking framework that combines adaptive clustering with predictive state estimation to ensure stable and reliable operation across varying conditions.

This research aims to design and implement a human tracking system based on FMCW radar by integrating adaptive Density Based Spatial Clustering of Applications with Noise (DBSCAN) clustering and the Kalman filter (KF). The system is developed to detect and track human targets in outdoor environments. Through this approach, the resulting framework not only improves reliability and efficiency but also adapts to the requirements of modern surveillance applications. The implementation is expected to provide a significant

contribution to the advancement of radar-based surveillance technology, particularly for robust operation in complex and dynamic outdoor scenarios.

2. MATERIAL AND METHOD

2.1 Proposed method

This study proposed a real-time human tracking system using an IWR6843ISK FMCW radar for outdoor environments. The radar detected human movement and generated three-dimensional point cloud data (x, y, z). Since the tracking is visualized in a top-view perspective, only the (x, y) coordinates are used for planar position estimation.

Before clustering, the point cloud was filtered using Signal-to-Noise Ratio (SNR) and Doppler velocity thresholds. This filtering step removes low-quality detections and static reflections, thereby reducing noise and ghost targets. The filtered 2D point cloud is clustered using DBSCAN to separate true targets from residual noise. Each cluster's centroid is then tracked using a KF, which performs predictive state estimation and measurement updates. This combination of filtering, density-based clustering, and predictive tracking enables accurate, stable, and robust performance in complex outdoor scenarios.

Beyond the overall system workflow shown in Figure 1, the adaptive DBSCAN module follows an internal processing sequence designed to adjust the clustering parameters based on range-dependent point cloud characteristics. This procedure is summarized in Figure 2, which outlines how the radar points are filtered, analyzed, and assigned to distance zones before the appropriate DBSCAN parameters are applied. The same workflow is also used during real-time operation, where each incoming frame is processed through this sequence to ensure that the adaptive ϵ and Minimum Points (MinPts) configuration remains effective under dynamic conditions and varying target ranges.

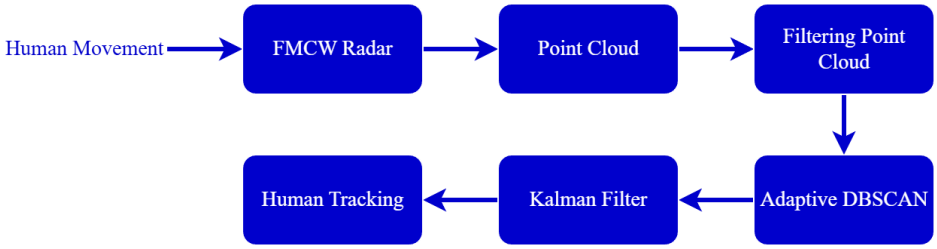

Figure 1. Proposed method

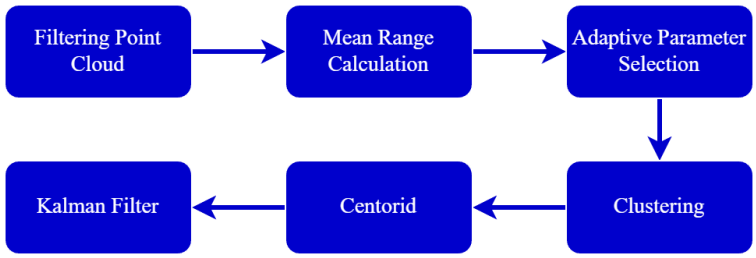

Figure 2. Adaptive Density-Based Spatial Clustering of Applications with Noise (DBSCAN) processing workflow

2.2 Frequency Modulated Continuous Wave radar

FMCW radar is a sensing technology that employs a sinusoidal waveform with linearly modulated frequency to measure the range and velocity of a target. The signal is transmitted as a chirp, in which the frequency increases gradually over a specified time interval and is reflected upon encountering an object [10].

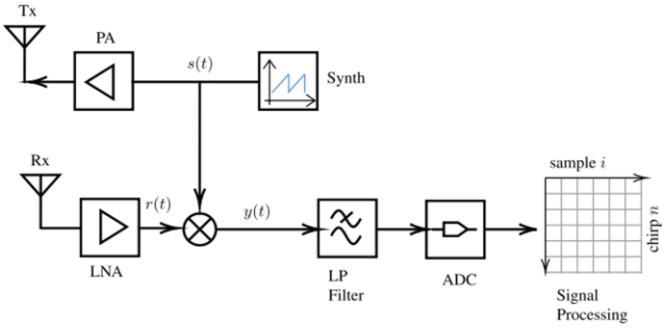

Figure 3. Main components of Frequency Modulated Continuous Wave (FMCW) radar [11]

The reflected signal is mixed with the newly transmitted signal to produce an intermediate frequency (IF) or beat frequency, which contains information on both target range and velocity. The range is determined from the signal's round-trip time, while the frequency shift caused by the Doppler effect is used to estimate the target's relative velocity [12]. The main components of the radar are illustrated in Figure 3.

2.3 Point cloud

A point cloud is a spatial data representation consisting of a set of points in three-dimensional (3D) space, where each point is defined by its (x, y, z) coordinates specifying its spatial position.

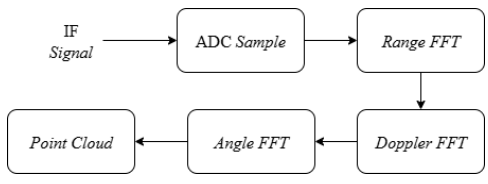

Figure 4. Point cloud generation process
Note: IF: intermediate frequency; FFT: Fast Fourier Transform; ADC: Analog to Digital Converter.

As illustrated in Figure 4, the generation of a point cloud involves a sequence of signal processing stages designed to extract the range, velocity, and angle of arrival from signals reflected by objects. The process begins with the IF signal, produced by mixing the transmitted and received radar signals, which is then digitized through an Analog to Digital Converter (ADC) sampling. The digitized data undergoes a range Fast Fourier Transform (FFT) to determine target distance, a Doppler FFT to estimate relative velocity, and an angle FFT to compute the angle of arrival. The combined results of these steps form a set of points describing the shape and motion of objects in 3D space. The detailed stages of this process are described as follows [12]:

(1). Range measurement

In FMCW radar systems, the distance to a target can be determined by analyzing the beat frequency, which arises from the difference between the transmitted chirp signal and its reflected echo. This beat frequency is directly related to the round-trip travel time of the signal between the radar and the object. The relationship can be expressed as Eq. (1):

$$R = \frac{c \times f_b}{2 \times S} \tag{1}$$

where, c is the speed of light 3×10^8 m/s, f_b is the measured beat frequency, and S represents the chirp slope. This formulation reflects the fact that the radar signal travels to the target and back, making the total path length twice the range being measured [12].

(2). Velocity measurement

In FMCW radar, the measurement of an object's velocity is based on the Doppler effect, which describes the change in frequency when an object moves relative to the radar. The Doppler frequency shift f_d is used to determine the object's radial velocity v with respect to the radar, expressed as Eq. (2):

$$v = \frac{\lambda \times f_d}{2} \tag{2}$$

where, λ denotes the wavelength of the transmitted radar signal. This relationship shows that the radial velocity can be directly calculated from the Doppler frequency shift caused by the object's relative motion with respect to the signal source [12].

(3). Angle measurement

The angle of arrival (θ) in FMCW radar is determined from the phase difference ($\Delta\varphi$) between signals received by adjacent antenna elements. It is calculated as:

$$\theta = sin^{-1}\left(\frac{\lambda \times \Delta\varphi}{2\pi \times d}\right) \tag{3}$$

where, λ is the wavelength and d is the spacing between antenna elements [12].

(4). Spatial coordinate conversion

A point cloud represents spatial data as a set of three-dimensional points (x, y, z) relative to the sensor [13]. In FMCW radar, the range R is obtained from beat frequency analysis, while the azimuth θ and elevation ϕ are determined from phase differences between antennas, and the target velocity is estimated from Doppler shifts. These parameters are then transformed into Cartesian coordinates using Eqs. (4)-(6) producing a 3D point cloud that represents the spatial position of detected targets [14].

$$x = R \times \cos(\theta) \times \cos(\phi) \tag{4}$$

$$y = R \times \sin(\theta) \times \cos(\phi) \tag{5}$$

$$z = R \times \sin(\phi) \tag{6}$$

2.4 Adaptive Density-Based Spatial Clustering of Applications with Noise

DBSCAN is a density-based clustering algorithm that groups data points into clusters when the number of points within a specified radius (ϵ) meets or exceeds a MinPts [15]. Points with at least MinPts neighbors are classified as core points, while points on the periphery of a cluster are classified as border points. Points that do not meet these criteria are considered noise.

In the context of FMCW radar, DBSCAN leverages the density and spatial distribution of point cloud data (x, y) to distinguish primary targets from environmental clutter. This approach enables the system to adaptively identify and separate objects from noise, thereby improving detection accuracy in a complex environment [16].

However, as the distance between the radar and the object increases, the reflected signal strength decreases due to propagation loss and beam spreading, leading to sparser point cloud distributions in the far-field region [17]. Consequently, a fixed choice ϵ and MinPts may not be suitable for all distances, as parameters optimised for dense near-field data can cause over-segmentation or missed detections in sparse regions. To address this, adaptive DBSCAN techniques dynamically adjust the values of ϵ and MinPts based on local point densities, distance-dependent thresholds, or statistical characteristics of radar reflections [18, 19].

2.5 Kalman filter

KF is used to refine the cluster centroids produced by the adaptive DBSCAN, providing a smoother and more stable target trajectory. The filter models human motion using a four-dimensional state vector $[x, y, v_x, v_y]^T$, describing the planar position and velocity of the target. A constant velocity motion model is adopted, and the state transition matrix is updated in real time based on the actual frame interval to accommodate variations in the radar sampling rate.

Radar measurements consist only of the position components [x, y], and are incorporated through a linear measurement model. The process noise covariance Q captures uncertainty in the motion model, while the measurement covariance R is adaptively adjusted based on the SNR of each detection. Higher SNR values correspond to more reliable measurements and thus a smaller R, whereas low SNR detections produce a larger covariance, reducing their influence on the filter update. This SNR-based adjustment helps the KF handle fluctuations in detection quality across different ranges.

The KF performs prediction and update steps at each frame to fuse the motion model with the incoming measurements. This approach effectively attenuates frame-to-frame jitter caused by uneven point density, intermittent point loss, or noisy detections, resulting in a smoother and temporally consistent trajectory suitable for subsequent analysis [5, 20].

3. EXPERIMENTAL SETUP AND PROCEDURE

Data collection was conducted in an outdoor environment using an FMCW IWR6843ISK radar operating at a frequency of 60 GHz, with an azimuth coverage of 120°. The radar was mounted at a height of 2 to 2.5 m above ground level and tilted downward at an elevation angle of approximately 2–5° as shown in Figure 5 to optimize the detection coverage area.

The data acquisition process involved several human movement scenarios to evaluate the tracking system's performance under various conditions. The first scenario was horizontal movement, where the subject moved laterally parallel to the radar at distances ranging from 5 m to 50 m, with data recorded at 5 m intervals as illustrated in Figure 6.

The second scenario was radial movement, in which the subject walked toward and away from the radar along the Y-axis for a distance of 50 m, to assess tracking robustness against range variations, as illustrated in Figure 7.

Additionally, a multi-angle tracking test was performed, where the subject moved in different directions with azimuth angles ranging from -60° to +60° relative to the radar position, as illustrated in Figure 8. This scenario aimed to evaluate the system's ability to recognize movement trajectories and assess position estimation accuracy from various viewing angles. All data were collected in real time as three-dimensional point clouds and served as the basis for evaluating the clustering and tracking algorithms.

Figure 5. Radar set-up position: (a) Radar tilt angle; (b) Radar height

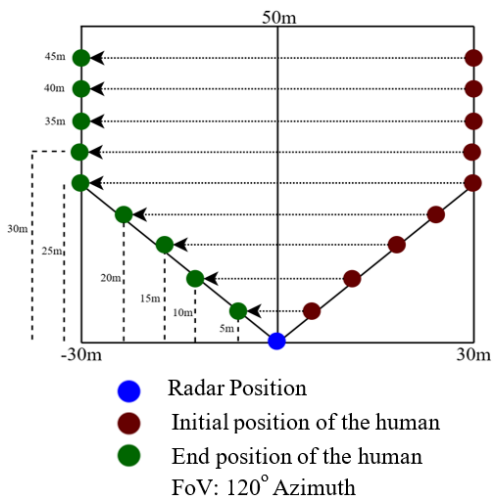

Figure 6. Horizontal movement

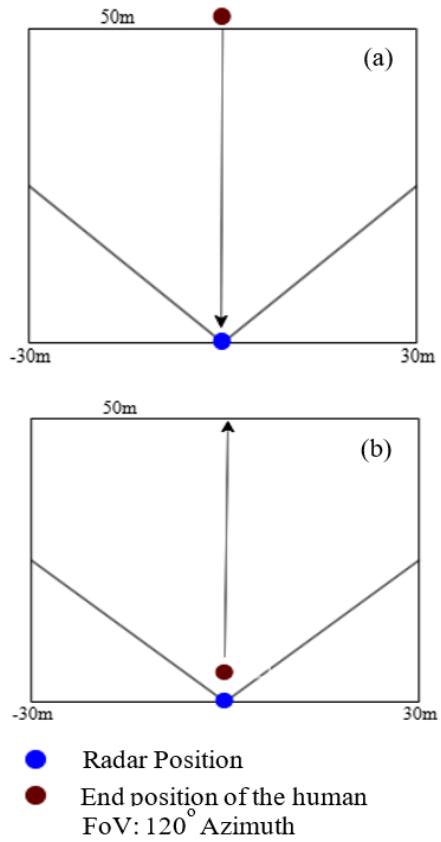

Figure 7. Radial movement: (a) Moves toward, (b) Away from the radar

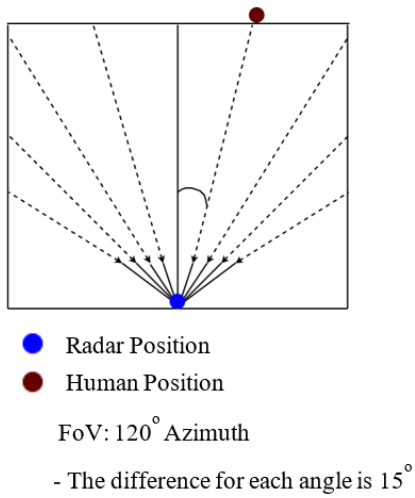

Figure 8. Multiangle movement

4. RESULT AND DISCUSSION

The experiments were conducted to assess the performance of the proposed FMCW radar-based tracking system, with the primary focus placed on evaluating the adaptive DBSCAN clustering mechanism. The analysis examines how the adaptive zoning strategy improves cluster formation across varying distances and contributes to stable trajectory estimation when combined with the KF. In addition to algorithmic evaluation, the experiments also verify the radar's tracking capability by measuring its effective detection range in real-time and comparing the estimated trajectory against a predefined reference path using Root Mean Square Error (RMSE).

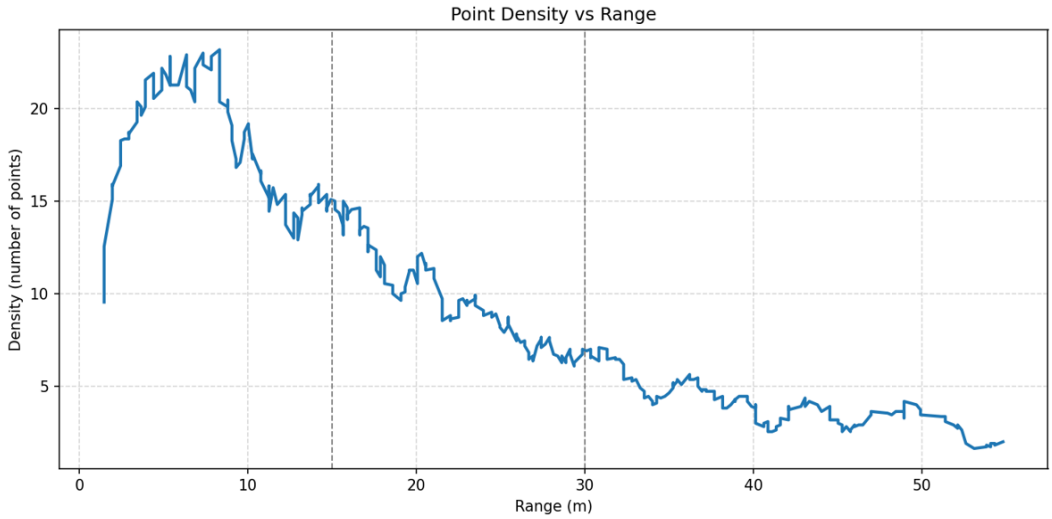

Figure 9. Point density vs. range

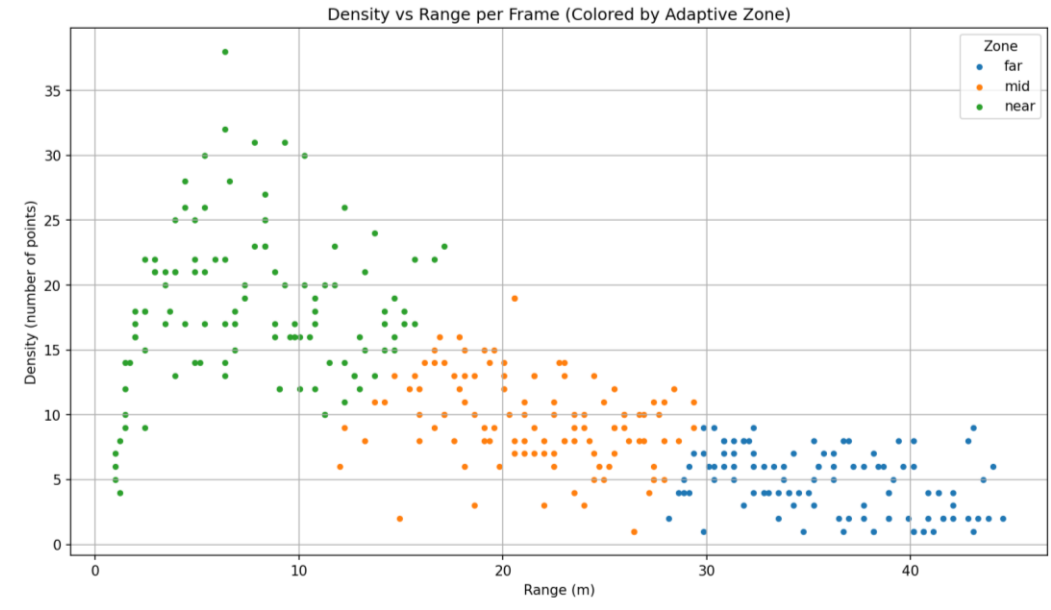

Figure 10. Density vs. range per frame

The performance of the DBSCAN algorithm is highly sensitive to the choice of its parameters, namely the neighborhood radius ϵ and the minimum number of points (MinPts). This sensitivity becomes a major challenge in radar point cloud data, where the spatial density of detections is non-uniform. Near targets tend to produce denser point returns due to stronger reflected power. In contrast, distant targets yield sparser point clouds as a result of propagation loss and signal attenuation [3]. As a consequence, a single set of DBSCAN parameters cannot consistently yield optimal clustering results across different ranges.

To address the density variation across distance, the behaviour of the collected point cloud data was first examined. Figure 9 shows the point density as a function of range, revealing a high-density region at short distances, a transitional region in the mid-range, and a sparse region beyond approximately 30 m.

This pattern is further confirmed in Figure 10, where the per-frame density plotted against the median range forms three naturally separated bands. These observations indicate that the measurement space does not vary uniformly but instead exhibits three distinct density regimes.

Based on this empirical evidence, a three-zone division was adopted, and K-Means clustering applied to the range density pairs produced the numerical boundaries summarized in Table 1. This zoning allows the DBSCAN parameters to adapt dynamically to the spatial density of the detections, improving clustering reliability across different ranges.

Table 1. Distance zone

Zone	Range (m)
Near	0–15
Medium	15.1–30
Far	30.1–50

Table 2. Parameter search range per zone

Zone	ε Value	Minimum Points (MinPts)
Near	0.10–0.80 (step 0.05)	3–10
Medium	0.20–1.50 (step 0.05)	2–8
Far	0.30–2.0 (step 0.1)	2–6

The parameter search ranges for each zone are listed in Table 2, where ε and MinPts were systematically varied using a grid search procedure. Since the dataset contains a single moving target, the quality of each parameter configuration was evaluated using a Cluster Count Accuracy (CCA), which measures how consistently DBSCAN produces exactly one cluster per frame, expressed as Eq. (7).

$$CCA(\%) = \left(\frac{\sum_{i=1}^{N} 1(C_i = 1)}{N}\right) \times 100\% \quad (7)$$

where,

N: the total number of frames;

C_i: the number of clusters produced in frame i;

$1(C_i = 1)$: an indicator function that returns 1 if frame i contains exactly one cluster, and 0 otherwise.

The parameter set yielding the highest proportion of correct single-cluster detections was selected as the optimal configuration for each zone.

Parameter tuning was performed using a grid search procedure, and each configuration was evaluated based on how consistently DBSCAN produced a single cluster per frame. The best performing settings for each zone are summarized in Table 3. The near zone yielded the highest stability due to its dense point returns, whereas the medium and far zones required larger ε values to accommodate the reduced point density at longer distances. These results confirm that the zone-based adaptation enables DBSCAN to maintain reliable clustering behaviour across varying ranges.

Table 3. Optimal Adaptive Density-Based Spatial Clustering of Applications with Noise parameters per zone

Zone	Epsilon (m)	MinPts	Accuracy
Near	0.650	4	98.21%
Medium	0.900	3	91.53%
Far	1.300	2	84.62%

Table 4. Evaluation at horizontal distances

Distance	Accuracy
5 m	95.74%
10 m	93.40%
15 m	90.32%
20 m	87.10%
25 m	84.37%
30 m	84.01%
35 m	82.51%
40 m	80.67%
45 m	50.77%
50 m	33.05%

Table 5. Cluster Count Accuracy evaluation in radial movements

Scenario	Accuracy
Approaching radar	87.50%
Receding radar	91.81%

Table 6. Centroid positions before tracking

Frame	Centroid		Cluster ID
	x	y	
25	-0.15	1.82	0
26	-0.16	1.95	0
27	-0.12	2.00	0
28	-0.07	2.33	0
29	-0.03	2.33	0

Table 7. Centroid positions after Kalman filter tracking

Frame	Centroid		Track ID
	x	y	
25	-0.14	1.84	4
26	-0.15	1.95	4
27	-0.12	2.01	4
28	-0.08	2.30	4
29	-0.03	2.35	4

This adaptive zoning strategy substantially improves the robustness of the clustering process by ensuring that the DBSCAN parameters are matched to the underlying density characteristics of each range segment. By doing so, it mitigates over-segmentation in the dense near field region and reduces the risk of missed detections in the sparser mid and far field regions. Consequently, the algorithm is able to generate stable and consistent single-cluster outputs across all distances. The optimized clustering results from each zone are then used as inputs to the KF for trajectory estimation, as discussed in the following subsection.

Before proceeding to trajectory estimation with the KF, the clustering performance of the adaptive DBSCAN algorithm was evaluated using the CCA, which measures how consistently the algorithm produces a single valid cluster per frame. Two experimental scenarios were considered: horizontal movement at distances ranging from 5 to 50 m, and radial movement in which the subject approached and receded along the Y-axis.

Table 4 shows that clustering performance is highest at close range, with CCA values of 95.74% at 5 m and 93.40% at 10 m. Accuracy gradually decreases as the subject moves farther away, reaching the mid 80% range at distances between 15 and 30 m. A more noticeable decline appears beyond 35 m, where accuracy drops to 82.51% at 35 m and 80.67% at 40 m. The performance then degrades sharply at the farthest distances, falling to 50.77% at 45 m and 33.05% at 50 m. This sharp decline is caused not only by increased noise but also by a significant loss of detections as the radar approaches its effective range limit. With fewer valid points available per frame, DBSCAN becomes increasingly difficult to maintain a consistent single-cluster output.

For the radial movement scenario, the adaptive DBSCAN also produced consistent clustering results, as shown in Table 5. When the subject moved toward the radar, the algorithm achieved an accuracy of 87.50%, while receding motion produced a slightly higher accuracy of 91.81%. These results indicate that the zone-based approach can effectively handle changes in point cloud distribution caused by different motion directions, allowing the clustering to remain reliable in both horizontal and radial movements.

Overall, the obtained results validate that the adaptive DBSCAN provides stable and accurate clustering across varying distances and movement patterns. However, despite the reliable formation of clusters, the centroid positions still exhibited minor frame-to-frame fluctuations due to noise and variations in the radar point cloud. To mitigate this effect and enhance temporal consistency, the KF was applied to refine the centroid trajectories, aiming to produce smoother and more stable motion estimation while preserving target identity.

In this stage, centroids from valid clusters were treated as measurement inputs for the KF-based tracking module. The KF performed recursive prediction and update steps for each detected object, enabling continuous tracking while maintaining consistent identity through frame-to-frame

association. The comparison presented in Tables 6 and 7 highlights this improvement. The raw centroids obtained from DBSCAN showed slight positional instability across consecutive frames, whereas the KF output produced smoother and more continuous trajectories with consistent Track IDs.

As shown in Tables 6 and 7, the raw centroids derived from DBSCAN exhibit minor frame-to-frame fluctuations caused by variations in the point cloud distribution. After KF filtering, the estimated trajectory becomes noticeably smoother and more stable, with the same track ID maintained throughout the sequence. This confirms that the KF effectively performs temporal smoothing and noise suppression while preserving object identity. Figure 11 further visualizes these effects, illustrating how the KF output provides a more coherent and continuous trajectory compared to the unfiltered clustering results.

To further quantify the tracking accuracy, the KF estimated trajectories were compared against predefined reference paths under controlled angular movements. To assess the overall tracking accuracy, the trajectories were evaluated against linear reference paths defined at nine azimuth angles ranging from -60° to 60°, in 15° increments. Each reference path was modeled as a straight line $y = mx$, where $m = \tan(\theta)$ and the radar was positioned at the origin (0,0). Figure 12 illustrates an example of the test setup at an azimuth angle of -15°, where the detected centroid trajectory is evaluated relative to the corresponding reference line.

For each frame, the perpendicular distance from the centroid to its corresponding reference line was calculated. The Mean Error and RMSE were then used as quantitative performance metrics, summarizing tracking accuracy across all azimuth directions. The results are presented in Table 8.

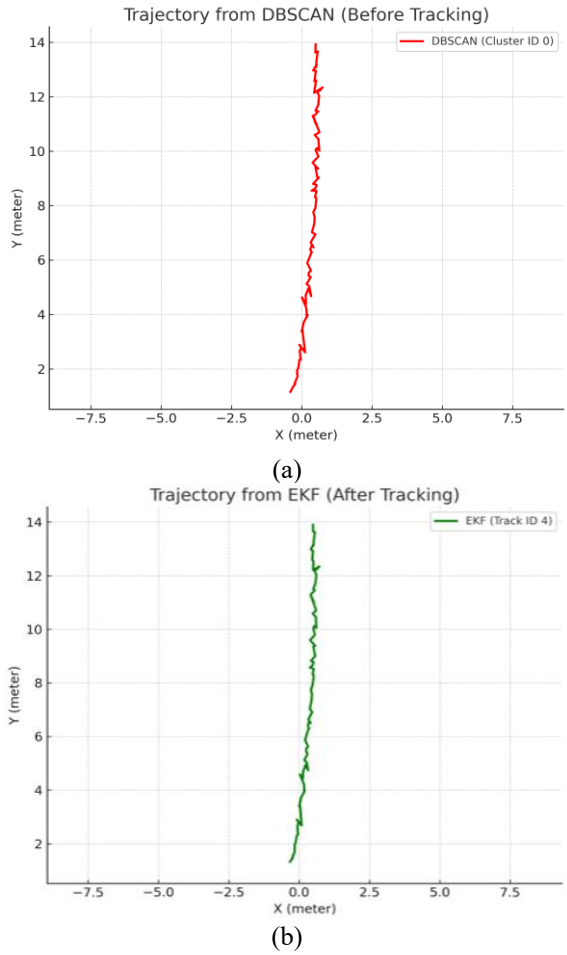

Figure 11. Trajectories before and after Kalman filter (KF) tracking: (a) without KF; (b) with KF

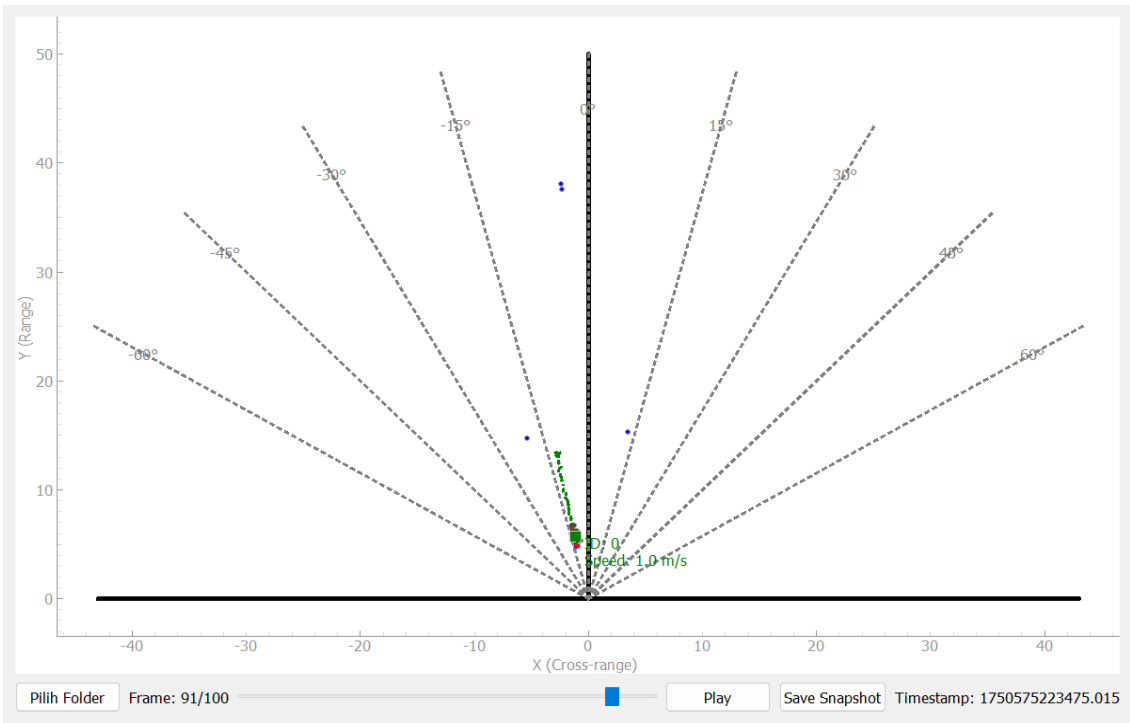

Figure 12. Example of trajectory evaluation at -15° reference angle

The results indicate that the system achieved the highest accuracy in the central azimuth directions (-15°, 0°, and 15°), where the RMSE values were as low as 0.23 m. This reflects stronger signal returns and higher point densities within the radar's main field of view. Conversely, larger errors were observed at wider angles (±45° and ±60°), where weaker

reflections and the edge effects of the radar's field of view reduced tracking precision, resulting in RMSE values exceeding 1 m.

Following the quantitative validation of the clustering and tracking algorithms, the system was further tested in a real-time outdoor environment to assess its practical performance under realistic operating conditions. The radar was mounted at a height of approximately 2–2.5 m with a slight downward tilt to align with the expected height of human subjects. Point cloud data were processed to detect and track human motion in real-time. Several scenarios were tested, including approaching and receding movements, lateral motion, and simultaneous tracking of multiple targets.

The evaluation focused on tracking success, defined as the ability of the system to consistently detect and maintain object trajectories across consecutive frames. The detection outcomes for different test scenarios are summarized in Table 9. The system reliably tracked both single and multiple human targets up to a distance of 35 m in both radial and horizontal motion scenarios. Beyond 40 m, continuous tracking could no longer be maintained, primarily due to signal attenuation and the reduced density of reflected points at longer distances.

These findings demonstrate that the proposed system achieves stable and accurate real-time human tracking up to 35 m under diverse conditions, while also highlighting the inherent limitations of mmWave radar performance beyond 40 m. This limitation is primarily caused by the radar's reduced detection capability at longer distances. As shown in Table 4, the clustering accuracy remains above 80% within the 5–35 m range but declines significantly beyond 40 m, reaching only 50.77% at 45 m and 33.05% at 50 m. At these distances, the point-cloud returns become sparse and increasingly noisy due to propagation loss and lower SNR, making it difficult for the system to form a stable cluster. Consequently, the decrease in tracking performance at farther ranges is attributed not to the filtering or validation strategy, but to the inherent sensing limitations of the radar itself.

Table 8. Tracking accuracy across reference angles

Reference Line Angle	Mean Error (m)	RMSE (m)
	0.2223	0.2296
0°	0.5662	0.5850
	0.6158	0.6487
	0.5097	0.5249
-15°	0.5324	0.5617
	0.4702	0.4990
	0.6453	0.6702
-30°	0.6490	0.6720
	0.6380	0.6551
	0.9811	0.9972
-45°	0.8455	0.9013
	0.9388	0.9898
	0.624	0.655
-60°	0.530	0.648
	0.747	0.893
	0.3354	0.3643
15°	0.2456	0.2895
	0.3569	0.3899
	0.6068	0.6715
30	0.5262	0.6115
	0.5581	0.6884
	0.7154	0.9422
45°	0.6837	0.8564
	0.663	0.828
	1.083	1.342
60	0.924	1.173
	0.720	0.857

Table 9. Real-time system evaluation

Scenario	Result
Approaching radar (≤ 35 m)	Detected
Receding from radar (≤ 35 m)	Detected
Three targets approaching	Detected
Two targets receding	Detected
Horizontal movement at 30 m	Detected
Receding from radar (40–50 m)	Not detected
Approaching radar (40–50 m)	Not detected

5. CONCLUSION

This study presented a real-time human tracking system using the IWR6843ISK FMCW radar by integrating adaptive DBSCAN clustering with KF-based trajectory estimation. The proposed adaptive zoning approach effectively addressed the range-dependent variation in point cloud density. Clustering evaluation using CCA showed that stable single cluster formation was maintained up to the mid-range distances, with accuracy remaining above 80% until approximately 35 m, before decreasing at farther ranges due to reduced SNR and point cloud sparsity. The radial movement tests supported these findings, with the adaptive method achieving consistent clustering performance for both approaching and receding motions. The KF further improved tracking stability by smoothing centroid fluctuations and producing continuous trajectories suitable for real-time operation. Overall, the combination of adaptive DBSCAN and KF provides a reliable and efficient framework for outdoor human tracking. The system performs robustly within the radar's effective operating range and demonstrates practical potential for surveillance and field deployment scenarios.

ACKNOWLEDGMENT

The authors would like to acknowledge the support from RIIM Kompetisi, funded by the Indonesia Endowment Fund for Education (LPDP), Ministry of Finance of Indonesia, and the National Research and Innovation Agency (BRIN) (Grant No.: 205/IV/KS/11/2023 and 369/SAM4/PPM/2023).

REFERENCES

[1] Zhang, L., Cao, L., Zhao, Z., Wang, D., Fu, C. (2024). A Crowd movement analysis method based on radar particle flow. Sensors, 24(6): 1899. https://doi.org/10.3390/s24061899

[2] Watanabe, T., Ma, Y., Huang, R. (2023). Multiple-person tracking with mmWave radar using adaptive clustering and ghost removing. In 2023 IEEE Smart World Congress (SWC), Portsmouth, United Kingdom, pp. 668-675. https://doi.org/10.1109/SWC57546.2023.10448562

[3] Haritha, J., Sowntharya, V., Kowshika, R., Hemavardhini, S. (2023). Investigation on Indoor Detection and Tracking of People using IWR1642 mmWave Sensor. In 2023 Third International Conference on Smart Technologies, Communication and Robotics (STCR), Sathyamangalam, India, pp. 1-6. https://doi.org/10.1109/STCR59085.2023.10396905

[4] Chen, W., Yang, H., Bi, X., Zheng, R., et al. (2023).

Environment-aware multi-person tracking in indoor environments with mmwave radars. Proceedings of the ACM on Interactive, Mobile, Wearable and Ubiquitous Technologies, 7(3): 89. https://doi.org/10.1145/3610902

[5] Santos, B., Oliveira, A.S., Carvalho, N.B., Fernandes, R., Cannizzaro, A., Cruz, P.M. (2021). FMCW radar point cloud multiperson tracking using a Kalman filter–based approach. URSI Radio Science Letters, 3: 68. https://doi.org/10.46620/21-0068

[6] Chowdhury, A., Pattnaik, N., Ray, A., Chakravarty, S., Chakravarty, T., Pal, A. (2023). Unobtrusive people identification and tracking using radar point clouds. IEEE Sensors Letters, 7(12): 1-4. https://doi.org/10.1109/LSENS.2023.3328794

[7] Pegoraro, J., Rossi, M. (2021). Real-time people tracking and identification from sparse mm-wave radar point-clouds. IEEE Access, 9: 78504-78520. https://doi.org/10.1109/ACCESS.2021.3083980

[8] Zhao, P., Lu, C.X., Wang, J., Chen, C., Wang, W., Trigoni, N., Markham, A. (2021). Human tracking and identification through a millimeter wave radar. Ad Hoc Networks, 116: 102475. https://doi.org/10.1016/j.adhoc.2021.102475

[9] Zhou, T.H., Xun, X., Wang, L., Hu, G., Ding, W., Kou, L. (2025). Self-adaptive clustering model based on variable time-series similarity measure analysis for V2G electricity price prediction. Applied Sciences, 15(4): 2069. https://doi.org/10.3390/app15042069

[10] Darlis, A.R., Ibrahim, N., Kusumoputro, B. (2021). Performance analysis of 77 GHz mmWave radar based object behavior. Journal of Communications, 16(12): 576-582. https://doi.org/10.12720/jcm.16.12.576-582

[11] Mafukidze, H.D., Mishra, A.K., Pidanic, J., Francois, S.W. (2022). Scattering centers to point clouds: A review of mmWave radars for non-radar-engineers. IEEE Access, 10: 110992-111021. https://doi.org/10.1109/ACCESS.2022.3211673

[12] Iovescu, C., Rao, S. (2017). The fundamentals of millimeter wave sensors. Texas Instruments. https://www.ti.com/lit/wp/spyy005a/spyy005a.pdf?ts=1773366970086.

[13] Soom, J., Leier, M., Janson, K., Tuhtan, J.A. (2024). Open urban mmWave radar and camera vehicle classification dataset for traffic monitoring. IEEE Access, 12: 65128-65140. https://doi.org/10.1109/ACCESS.2024.3397013

[14] Richards, M.A. (2005). Fundamentals of Radar Signal Processing. New York: Mcgraw-Hill.

[15] Khan, N.F. (2024). Movement detection of people in indoor spaces with radar sensors. Doctoral dissertation, Politecnico di Torino.

[16] Id, I.D., Mahdiyah, E. (2017). Modifikasi DBSCAN (density-based spatial clustering with noise) pada objek 3 dimensi. Jurnal Komputer Terapan, 3(1): 41-52. https://doi.org/10.13140/RG.2.2.22346.67529

[17] Fioranelli, F., Ritchie, M., Griffiths, H. (2016). Performance analysis of centroid and SVD features for personnel recognition using multistatic micro-Doppler. IEEE Geoscience and Remote Sensing Letters, 13(5): 725-729. https://doi.org/10.1109/LGRS.2016.2539386

[18] El Yabroudi, M., Awedat, K., Chabaan, R.C., Abudayyeh, O., Abdel-Qader, I. (2022). Adaptive DBSCAN LiDAR point cloud clustering for autonomous driving applications. In 2022 IEEE International Conference on Electro Information Technology (eIT), Mankato, MN, USA, pp. 221-224. https://doi.org/10.1109/eIT53891.2022.9814025

[19] Wang, C., Ji, M., Wang, J., Wen, W., Li, T., Sun, Y. (2019). An improved DBSCAN method for LiDAR data segmentation with automatic Eps estimation. Sensors, 19(1): 172. https://doi.org/10.3390/s19010172

[20] Ribeiro, M. I. (2004). Kalman and extended Kalman filters: Concept, derivation and properties. Institute for Systems and Robotics, 43(46): 736-3741.